PERGAMON

International Journal of Heat and Mass Transfer 46 (2003) 939–948

International Journal of HEAT and MASS TRANSFER

www.elsevier.com/locate/ijhmt

# On the stability analysis of thermally stratified channel flow with a compliant boundary

Sandile S. Motsa [a,*], P. Sibanda [b]

[a] Department of Mathematics, University of Swaziland, Private Bag 4, Kwaluseni, Swaziland
[b] Department of Mathematics, University of Zimbabwe, P.O. Box MP 167, Mount Pleasant, Harare, Zimbabwe

Received 14 August 2002; received in revised form 23 September 2002

**Abstract**

In this work we investigate the linear viscous stability of thermally stratified plane Poiseuille channel flow over a compliant surface. This problem is posed as an 'Orr–Sommerfeld-like' eigenvalue problem which is coupled to an energy equation. The Chebyshev collocation spectral method is used to solve the eigenvalue system. The critical Reynolds numbers, wavenumbers, wavespeeds, and curves of neutral stability are obtained for a wide range of compliant wall parameters and buoyancy parameters. These results are discussed and compared with results from related studies on thermally stratified flow between rigid flat plates (plane Poiseuille flow).


## 1. Introduction

In this paper we consider the stability of flow with a parabolic velocity profile between two walls (the upper wall being solid and the lower wall is compliant). The walls of the channel are maintained at different temperatures to create a temperature gradient (and buoyancy) in the flow field.

The work presented here is an extension of the work of Gage and Reid [8] to include wall compliance. Gage and Reid [8] investigated the stability of thermally stratified plane Poiseuille flow in a channel with rigid walls. This work was later extended to other velocity profiles (asymptotic suction boundary layer and an inflexion-point profile) by Gage [7]. By plotting marginal stability curves using fixed values of a dimensionless buoyancy parameter, the Richardson number ($Ri$), Gage and Reid [8] and Gage [7] showed that the flow is rendered stable by the application of a sufficiently strong thermal stratification and rendered unstable in the case of unstable stratification. The theory of Gage and Reid [8] predicts that when $Ri > 0.0554$ the flow will be stable and when $Ri < 0.0554$ the flow will be unstable to small disturbances. The results of Gage [7] confirmed this conclusion qualitatively, although the numerical values were different from the results of Gage and Reid [8].

Further theoretical work on the stability of thermally stratified viscous flow can be found in Herwig [10], Herwig and Schäfer [11], Schäfer and Herwig [16], Schäfer et al. [17] and Severin and Herwig [18] who considered the effects of temperature dependent viscosity on boundary layers and channel flows [16], Denier and Mureithi [6], who considered weakly nonlinear wave motions in a thermally stratified boundary layer; Denier and Bassom [5] who worked on the influence of thermal buoyancy on neutral wave modes in Poiseuille–Couette flow. In all the afore-mentioned works the governing momentum and energy equations were solved subject to the usual "no-slip" boundary conditions for rigid walls. In the current work we extend this problem to include compliant boundaries. The introduction of wall compliance in channel flows leads to stabilization of Tollmien–Schlichting instability waves (see for example [4]). This is the motivation to include wall compliance in the current problem. The geometry of the problem under study consists of a channel with one flexible wall and the other being rigid. The main aim of this work is to

* Corresponding author.
*E-mail addresses:* sandile@science.uniswa.sz (S.S. Motsa), sibanda@maths.uz.ac.zw (P. Sibanda).

0017-9310/03/$ - see front matter 
PII: S0017-9310(02)00377-0

describe the influence of wall compliance on the Tollmien–Schlichting instability waves in channel flows with thermal stratification using the numerical Chebyshev spectral collocation method.

Results from the numerical analysis of this work illustrate the delicate physical and mathematical balances controlling the Tollmien–Schlichting instabilities and may have medical applications. For example, rigid inserts are sometimes used to reinforce blood vessels in the treatment of cardiovascular diseases. The present work may also be of relevance in technological applications such as membrane bio-reactors, bio-mechanics and in other pipe flow situations where stable laminar flows are preferred (for example in the modelling of flow of body fluids in the human body).

In the following sections the mathematical problem is formulated, the numerical method of solution is outlined and the results are presented graphically and discussed qualitatively. A conclusion based on the summary of our findings is also presented.

## 2. Mathematical formulation

We consider the flow of a viscous incompressible fluid confined between the planes $y = \pm L/2$. When the effects of buoyancy are considered, the equations governing such a flow are the usual Navier–Stokes and energy equations under the Boussinesq approximation. The governing equations may be nondimensionalized in terms of the channel half width, the undisturbed centreline speed and half the prescribed temperature difference between the two boundary walls. The lower wall is compliant and the upper wall is rigid. The flow quantities representing properties of small disturbances introduced to the basic flow are assumed to be proportional to $\exp \mathrm{i}\alpha(x - ct)$, where $x$ is the streamwise direction of the flow, $\alpha$ is the wavenumber and $c$ is the wavespeed. The governing linearized equations (see [5,7,8,12]) are

$$\mathrm{i}\alpha(U_\mathrm{B} - c)u + v\frac{\mathrm{d}U_\mathrm{B}}{\mathrm{d}y} = -\mathrm{i}\alpha p + \frac{1}{Re}\left(\frac{\mathrm{d}^2u}{\mathrm{d}y^2} - \alpha^2 u\right), \tag{1}$$

$$\mathrm{i}\alpha(U_\mathrm{B} - c)v = -\frac{\mathrm{d}p}{\mathrm{d}y} + \frac{1}{Re}\left(\frac{\mathrm{d}^2v}{\mathrm{d}y^2} - \alpha^2 v\right) + G\theta, \tag{2}$$

$$\mathrm{i}\alpha(U_\mathrm{B} - c)\theta + v\frac{\mathrm{d}\theta_\mathrm{B}}{\mathrm{d}y} = \frac{1}{PrRe}\left(\frac{\mathrm{d}^2\theta}{\mathrm{d}y^2} - \alpha^2\theta\right), \tag{3}$$

$$\mathrm{i}\alpha u + \frac{\mathrm{d}v}{\mathrm{d}y} = 0. \tag{4}$$

The quantities $u$, $v$, $\theta$ and $p$ are respectively the streamwise velocity, normal velocity, temperature and pressure. The variable $y$ is the direction normal to the walls. The Reynolds number is defined by $Re = UL/2\nu$ and $Pr$ is the Prandtl number defined as $Pr = \nu/\kappa$ with $L$ being the channel half width, $\nu$ is the kinematic viscosity, $U$ is the centre-line speed and $\kappa$ is the coefficient of thermal diffusivity. The parameter $G$ is a buoyancy parameter defined by $G = GrRe^{-3/2}$ where $Gr$ is the Grashof number defined as $Gr = g\beta L^3\Delta\theta/\nu^2$ where $g$ is the acceleration due to gravity, $\beta$ is the coefficient of volume expansion, and $\Delta\theta$ is the temperature difference between the two walls. In the present problem, we assume that the basic velocity and temperature profiles have the simple forms $U_\mathrm{B} = 1 - y^2$ and $\theta_\mathrm{B} = y$ respectively. In terms of nondimensional variables the boundaries of the channel are located at $y = \pm 1$ when the mean flow is undisturbed.

By introducing the stream function $\psi(x, y, t) = \phi(y)\exp[\mathrm{i}\alpha(x - ct)]$ in the continuity equation (4), the velocity components can be written in terms of the disturbance profile as $u = \phi'(y)$, $v = -\mathrm{i}\alpha\phi$. Using this definition in Eqs. (1)–(3) we can eliminate $u$, $v$ and $p$ to obtain

$$(U_\mathrm{B} - c)(\phi'' - \alpha^2\phi) - U_\mathrm{B}''\phi = \frac{1}{\mathrm{i}\alpha Re}(\phi'''' - 2\alpha^2\phi'' + \alpha^4\phi) - G\theta, \tag{5}$$

$$(U_\mathrm{B} - c)\theta + \theta_\mathrm{B}'\phi = \frac{1}{\mathrm{i}\alpha RePr}(\theta'' - \alpha^2\theta), \tag{6}$$

where the primes denote differentiation with respect to $y$.

## 3. Wall model and boundary conditions

We model the flexible wall as a spring-backed elastic plate similar to that of Carpenter and Garrad [2] so that the mechanical fluid pressure $p_\mathrm{w}$ due to the normal displacement of the compliant surface $\eta$ is given in dimensionless form as

$$p_\mathrm{w} = \frac{T}{Re^2}\frac{\partial^2\eta}{\partial x^2} - M\frac{\partial^2\eta}{\partial t^2} - \frac{d}{Re}\frac{\partial\eta}{\partial t} - \frac{B}{Re^2}\frac{\partial^4\eta}{\partial x^4} - \frac{K\eta}{Re^2}, \tag{7}$$

where $M$, $d$, $B$, $T$ and $K$ are the nondimensional plate mass, damping coefficient, flexural rigidity, tension and equivalent spring stiffness respectively. Details about the derivation and the nondimensionalization leading to Eq. (7) are given in ([2,4,9,15] for example).

If we express the wall displacement in normal mode form as $\eta = \tilde{\eta}\mathrm{e}^{\mathrm{i}\alpha(x-ct)}$, we can write the linearized boundary conditions at the compliant wall as

$$\phi'(-1) + \eta U_\mathrm{B}'(-1) = 0, \tag{8}$$

$$\phi(-1) - c\eta = 0, \tag{9}$$

$$\theta(-1) = 0. \tag{10}$$

Eliminating $\eta$ in Eqs. (8)–(10) gives

$$c\phi'(-1) + U_\mathrm{B}'(-1)\phi(-1) = 0. \tag{11}$$

Using the $x$-momentum equation (1), we infer that the boundary condition for the pressure at the lower wall is

$$p_w(-1) = \frac{1}{i\alpha Re}[\phi'''(-1) - \alpha^2\phi'(-1)]. \quad (12)$$

From (7), (9), (12) we obtain

$$\left[-\left(M\alpha^2c^2 + \frac{id\alpha c}{Re}\right) + \frac{1}{Re^2}(B\alpha^4 + T\alpha^2 + K)\right]\phi(-1) = \frac{ic}{\alpha Re}[\phi'''(-1) - \alpha^2\phi'(-1)]. \quad (13)$$

The remaining boundary conditions for the rigid upper wall are

$$\phi(1) = \phi'(1) = \theta(1) = 0. \quad (14)$$

Eqs. (5), (6), (11), (13), and (14) form an eigenvalue problem

$$\mathscr{L}(\alpha, c, Re, G) = 0, \quad (15)$$

that must be solved for the complex eigenvalue, $c = c_r + ic_i$ for fixed values of $Re$, $Pr$, $d$, $T$, $K$, $M$, $B$, $G$ and $\alpha$.

It is a well established fact in fluid mechanics that the disturbances are temporally growing if the wavenumber, $\alpha$ is real and the wavespeed, $c$ is complex. When $\alpha$ is complex and $c$ is real, the disturbance waves are spatially growing. Both temporally and spatially growing modes are of significance in the study of Tollmien–Schlichting instabilities found in flows over rigid and compliant surfaces. In this study, however, we restrict ourselves to temporally growing neutral modes.

For a given basic velocity profile $U(y)$, one or more neutrally stable modes may be present. The $(\alpha, Re)$ plane may then be divided into regions where $c_i < 0$ and regions where $c_i > 0$. These regions are separated by the the marginal stability curve $c_i(\alpha, Re, G) = 0$. Marginal stability curves are obtained by finding solutions of Eq. (15) for which both $\alpha$ and $c$ are real. To establish that these marginal stability curves represent the stability boundaries, it is necessary to show that $c_i$ changes sign when crossing the marginal stability curve.

We note that the eigenvalue problem will be nonlinear in the eigenvalue $c$ because of the boundary condition (13). Without loss of generality, the nonlinearity in the problem can be avoided by setting $M = 0$ in Eq. (13). The case when $M \neq 0$ was considered by Davies and Carpenter [4] in a related problem.

## 4. Solution method

To solve the eigenvalue system we adopt the Chebyshev spectral collocation method. We expand the solutions of the governing equations (5) and (6) together with the boundary conditions (11), (13) and (14) as truncated series of Chebyshev polynomials

$$\phi(y) = \sum_{k=0}^{N} \tilde{\phi}_k T_k(y), \quad (16)$$

$$\theta(y) = \sum_{k=0}^{N} \tilde{\theta}_k T_k(y), \quad (17)$$

where $T_k$ is the $k$th Chebyshev polynomial and $\tilde{\phi}_k$ and $\tilde{\theta}_k$ are the Chebyshev coefficients. Inserting Eqs. (16) and (17) into the governing equations we obtain a linear eigenvalue system of the form

$$\begin{pmatrix} A^{(0)} & A^{(1)} \\ B^{(0)} & B^{(1)} \end{pmatrix}\begin{pmatrix} \Phi \\ \Theta \end{pmatrix} = c\begin{pmatrix} A^{(2)} & \mathbf{O}_1 \\ \mathbf{O}_2 & B^{(2)} \end{pmatrix}\begin{pmatrix} \Phi \\ \Theta \end{pmatrix}, \quad (18)$$

where

$$\Phi^t = (\tilde{\phi}_0, \tilde{\phi}_1, \ldots, \tilde{\phi}_{N-1}, \tilde{\phi}_N),$$
$$\Theta^t = (\tilde{\theta}_0, \tilde{\theta}_1, \ldots, \tilde{\theta}_{N-1}, \tilde{\theta}_N),$$
$$A^{(0)} = \mathbf{U}_B(\mathbf{D}^2 - \alpha^2\mathbf{I}) - \mathbf{U}_B'' + \frac{i}{\alpha Re}(\mathbf{D}^4 - 2\alpha^2\mathbf{D}^2 + \alpha^4\mathbf{I}),$$
$$A^{(1)} = G\mathbf{I},$$
$$A^{(2)} = \mathbf{D}^2 - \alpha^2\mathbf{I},$$
$$B^{(0)} = \Theta_B',$$
$$B^{(1)} = \mathbf{U}_B + \frac{i}{\alpha RePr}(\mathbf{D}^2 - \alpha^2\mathbf{I}),$$
$$B^{(2)} = \mathbf{I}.$$

Here the superscript t represents the transpose, $\mathbf{I}$ is an $(N+1)\times(N+1)$ identity matrix, $\mathbf{O}_1$ and $\mathbf{O}_2$ are $(N+1)\times(N+1)$ matrices of zeros and $\mathbf{D}$ is the standard matrix differentiation operator defined in Canuto et al. [1]. The vectors $\mathbf{U}_B, \mathbf{U}_B''$ and $\Theta_B'$ are the values of $U_B$, $U_B''$ and $\theta_B'$ evaluated at the collocation points and placed on the main diagonal of an $(N+1)\times(N+1)$ matrix of zeros. The collocation points used are the Gauss–Lobatto points defined by

$$y_j = \cos\frac{\pi j}{N}, \quad -1 \leqslant y \leqslant 1, \quad j = 0, 1, \ldots, N. \quad (19)$$

The boundary conditions are given by

$$\tilde{\phi}_0 = \tilde{\theta}_0 = 0, \quad (20)$$

$$\sum_{k=0}^{N} D_{0k}\tilde{\phi}_k = 0, \quad (21)$$

$$c\sum_{k=0}^{N} D_{Nk}\tilde{\phi}_k + U_B'(-1)\tilde{\phi}_N = 0, \quad (22)$$

$$\tilde{\theta}_N = 0, \quad (23)$$

$$c\left[-\frac{\mathrm{i}}{\alpha Re}\sum_{k=0}^{N}\left(\mathbf{D}_{Nk}^{3}-\alpha^{2}\mathbf{D}_{Nk}\right)\tilde{\phi}_{k}-\frac{\mathrm{i}d\alpha}{Re}\tilde{\phi}_{N}\right]+\frac{1}{Re^{2}}(B\alpha^{4}+T\alpha^{2}+K)\tilde{\phi}_{N}=0. \tag{24}$$

Since $\tilde{\phi}_0$ and $\tilde{\theta}_0$ are known from Eq. (20) we infer that the matrices $A_{jk}^{(i)}$ and $B_{jk}^{(i)}$ $(i=0,1,2)$ and the boundary conditions (21)–(24) need only be satisfied for $j,k=1,2,\ldots N$. Also, because $\tilde{\theta}_N$ is given explicitly in Eq. (23), the matrices $A^{(1)}$, $B^{(1)}$, $B^{(2)}$ and $\mathbf{O}_1$ must be satisfied for $j=1,2,\ldots,N$, $k=1,2,\ldots,N-1$. This amounts to deleting the appropriate rows and columns of the differentiation matrix. The remaining boundary conditions are incorporated in the original second, $(N-1)$th and $N$th rows of $A^{(i)}$ $(i=0,1,2)$ and second, $(N-1)$th rows of $B^{(i)}$ as illustrated in the matrix equation below:

$$\begin{bmatrix}
\mathbf{D}_{01} & \mathbf{D}_{02} & \cdots & \mathbf{D}_{0N-1} & \mathbf{D}_{0N} & \vdots & 0 & 0 & \cdots & 0 & 0 \\
 & & \tilde{\mathbf{A}}_{(0)} & & & \vdots & & & \tilde{\mathbf{A}}_{(1)} & & \\
0 & 0 & \cdots & 0 & -\frac{S}{Re^{2}} & \vdots & 0 & 0 & \cdots & 0 & \\
0 & 0 & \cdots & 0 & -U_{\mathrm{B}}'(-1) & \vdots & 0 & 0 & \cdots & 0 & 0 \\
\cdots & \cdots & \cdots & \cdots & \cdots & \cdots & \cdots & \cdots & \cdots & \cdots & \cdots \\
 & & & & & \vdots & & & & & \\
 & & \widetilde{\mathbf{B}}_{(0)} & & & \vdots & & & \widetilde{\mathbf{B}}_{(1)} & & \\
 & & & & & \vdots & & & & &
\end{bmatrix}
\begin{bmatrix}
\tilde{\phi}_1 \\ \tilde{\phi}_2 \\ \vdots \\ \tilde{\phi}_{N-1} \\ \tilde{\phi}_N \\ \cdots \\ \tilde{\theta}_1 \\ \vdots \\ \tilde{\theta}_{N-1}
\end{bmatrix}$$

$$= c\begin{bmatrix}
0 & 0 & \cdots & 0 & 0 & \vdots & 0 & 0 & \cdots & 0 & 0 \\
 & & \tilde{\mathbf{A}}_{(2)} & & & \vdots & 0 & 0 & \cdots & 0 & 0 \\
 & & & & & \vdots & \vdots & \vdots & \vdots & \vdots & \vdots \\
BC2 & BC2 & BC2 & BC2 & bc2 & \vdots & 0 & 0 & \cdots & 0 & 0 \\
\mathbf{D}_{N1} & \mathbf{D}_{N2} & \cdots & \mathbf{D}_{NN-1} & \mathbf{D}_{NN} & \vdots & 0 & 0 & \cdots & 0 & 0 \\
\cdots & \cdots & \cdots & \cdots & \cdots & \cdots & \cdots & \cdots & \cdots & \cdots & \cdots \\
0 & 0 & \cdots & 0 & 0 & \vdots & & & & & \\
\vdots & \vdots & \vdots & \vdots & \vdots & \vdots & & & \widetilde{\mathbf{B}}_{(2)} & & \\
0 & 0 & \cdots & 0 & 0 & \vdots & & & & &
\end{bmatrix}
\begin{bmatrix}
\tilde{\phi}_1 \\ \tilde{\phi}_2 \\ \vdots \\ \tilde{\phi}_{N-1} \\ \tilde{\phi}_N \\ \cdots \\ \tilde{\theta}_1 \\ \vdots \\ \tilde{\theta}_{N-1}
\end{bmatrix},$$

which can be written as the generalized eigenvalue problem

$$\mathbf{EY}=c\mathbf{FY}, \tag{25}$$

where

$$\mathbf{Y}=(\tilde{\phi}_1,\ldots,\tilde{\phi}_N,\tilde{\theta}_1,\ldots,\tilde{\theta}_{N-1})^{\mathrm{t}},$$

$$BC2=-\frac{\mathrm{i}}{\alpha Re}\sum_{k=1}^{N-1}(\mathbf{D}_{Nk}^{3}-\alpha^{2}\mathbf{D}_{Nk}),$$

$$bc2=-\frac{\mathrm{i}}{\alpha Re}(\mathbf{D}_{NN}^{3}-\alpha^{2}\mathbf{D}_{NN})-\frac{\mathrm{i}d\alpha}{Re},$$

$$S=B\alpha^{4}+T\alpha^{2}+K.$$

The matrices $\tilde{\mathbf{A}}_{(i)}$ $(i=0,2)$ and $\widetilde{\mathbf{B}}_{(0)}$ are obtained by evaluating the original matrices $A_{jk}^{(i)}$ for $j=2,\ldots N-2$, $k=1,\ldots,N$ and $B_{jk}^{(i)}$ for $j=1,\ldots N-1$, $k=1,\ldots,N$. Similarly, $\tilde{\mathbf{A}}_{(1)}$, $\widetilde{\mathbf{B}}_{(1)}$ and $\widetilde{\mathbf{B}}_{(2)}$ are obtained by calculating $A_{jk}^{(1)}$ for $j=2,\ldots,N-2$, $k=1,\ldots,N-1$ and $B_{jk}^{(i)}$ $(i=1,2)$ for $j=k=1,\ldots,N-1$.

It can be seen that the matrix $\mathbf{F}$ in Eq. (25) is singular. If the generalized eigenvalue problem (25) is evaluated as it is, physically meaningless eigenmodes of infinitely large magnitude which interfere with the desired eigenmodes are obtained. This problem can be overcome by eliminating $\tilde{\phi}_1$ by using the boundary condition (21) to obtain

$$\tilde{\phi}_1=-\frac{1}{\mathbf{D}_{01}}\left[\mathbf{D}_{02}\tilde{\phi}_2+\mathbf{D}_{03}\tilde{\phi}_3+\cdots+\mathbf{D}_{0N-1}\tilde{\phi}_{N-1}+\mathbf{D}_{0N}\tilde{\phi}_N\right], \tag{26}$$

which is used to eliminate the first rows and first columns of $\mathbf{E}_{jk}$ and $\mathbf{F}_{jk}$ $(j,k = 1,\ldots,2N-1)$. This is done by defining

$$\mathscr{E}_{11} = E_{11},$$
$$\mathscr{E}_{12} = E_{jk} \quad (j = 1; k = 2,3,\ldots,2N-1),$$
$$\mathscr{E}_{21} = E_{jk} \quad (j = 2,3,\ldots,2N-1; k = 1),$$
$$\mathscr{E}_{22} = E_{jk} \quad (j = k = 2,3,\ldots,2N-1),$$
$$\mathscr{F}_{11} = F_{11},$$
$$\mathscr{F}_{12} = F_{jk} \quad (j = 1; k = 2,3,\ldots,2N-1),$$
$$\mathscr{F}_{21} = F_{jk} \quad (j = 2,3,\ldots,2N-1; k = 1),$$
$$\mathscr{F}_{22} = F_{jk} \quad (j = k = 2,3,\ldots,2N-1),$$
$$Y_1 = \tilde{\phi}_1,$$
$$Y_2 = \tilde{\phi}_2,\ldots,\tilde{\phi}_N,\tilde{\theta}_1,\ldots,\tilde{\theta}_{N-1}.$$

Using the above definitions, we can partition Eq. (25) as follows:

$$\mathscr{E}_{11}Y_1 + \mathscr{E}_{12}Y_2 = 0, \tag{27}$$

$$\mathscr{E}_{21}Y_1 + \mathscr{E}_{22}Y_2 = c\mathscr{F}_{21}Y_1 + c\mathscr{F}_{22}Y_2. \tag{28}$$

Eq. (27) can then be solved for $Y_1$ in terms of $Y_2$ as $Y_1 = -\mathscr{E}_{11}^{-1}\mathscr{E}_{12}Y_2$ and this result is substituted into Eq. (28) to give the $(2N-2)\times(2N-2)$ matrix eigenvalue system

$$\widetilde{\mathbf{E}}Y_2 = c\widetilde{\mathbf{F}}Y_2, \tag{29}$$

where $\widetilde{\mathbf{E}} = \mathscr{E}_{22} - \mathscr{E}_{21}\mathscr{E}_{11}^{-1}\mathscr{E}_{12}$ and $\widetilde{\mathbf{F}} = \mathscr{F}_{22} - \mathscr{F}_{21}\mathscr{E}_{11}^{-1}\mathscr{E}_{12}$. Note that (29) does not suffer from $\widetilde{\mathbf{F}}$ being singular. Hence its eigenvalues can be computed efficiently by first multiplying (29) by the inverse of $\widetilde{\mathbf{F}}$ to give

$$(\widetilde{\mathbf{F}}^{-1}\widetilde{\mathbf{E}} - c\mathbf{I}_1)Y_2 = 0, \tag{30}$$

where $\mathbf{I}_1$ is an identity matrix of size $(2N-2)\times(2N-2)$.

There exist many standard numerical methods to solve equations like (29) and (30). Here we used the generalized eigenvalue solver *eig* which is embodied into the commercially available software, MATLAB.

## 5. Results

The stability characteristics of the flow are obtained by solving the eigenvalue problem (29). The results presented here were obtained when $N = 70$ and $Pr = 1$ and for different values of the buoyancy and wall parameters.

The numerical scheme used in the study was validated by computing the most unstable eigenmode when $Re = 10000$, $\alpha = 1$, $G = 0$, $K = B = T = 1\times10^{11}$. This choice of large wall parameters reduces the problem to that of the rigid wall case. The most unstable eigenvalue for this choice of parameters was found to be $c = 0.2375 + 0.0037i$. This value corresponds to the

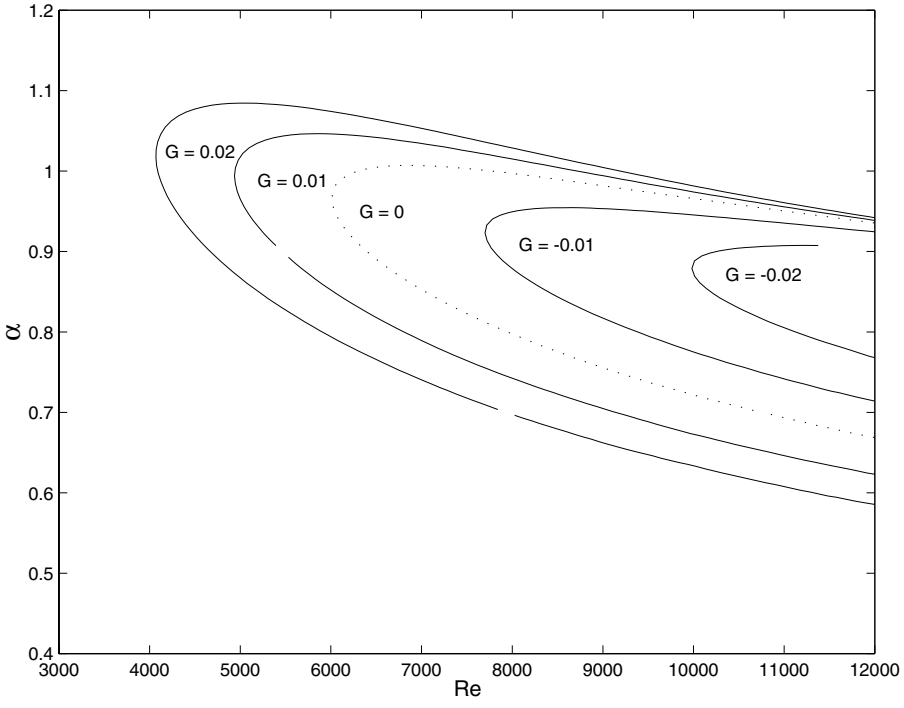


Fig. 1. Marginal stability curve for $B = T = K = 1\times10^7$, $d = 0$, $G = -0.02, -0.01, 0, 0.01, 0.02$.

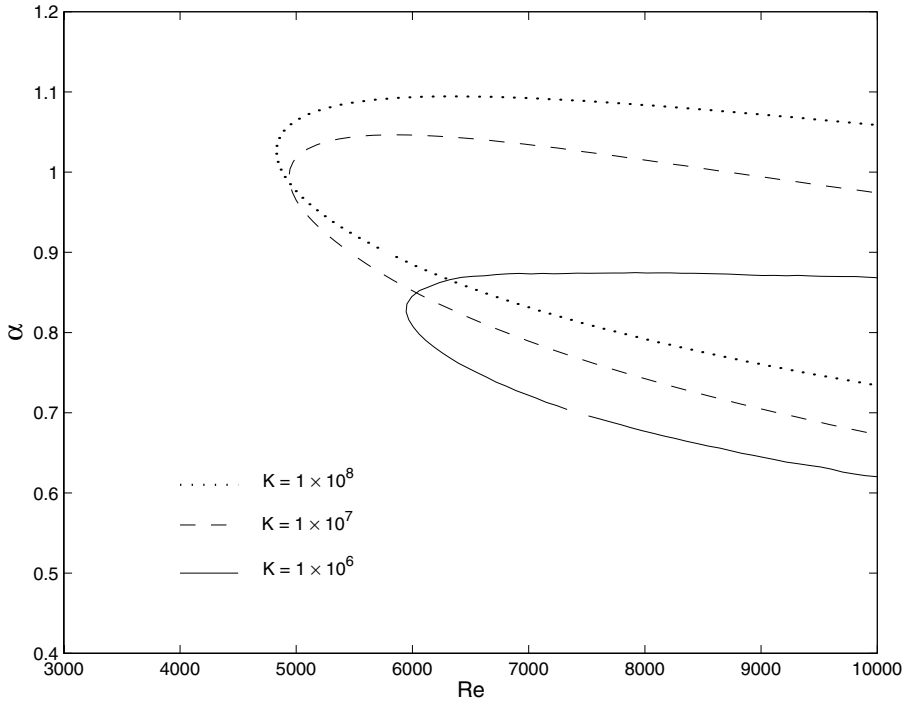


Fig. 2. Marginal stability curve for $T = B = 1 \times 10^7$, $d = 0$, $G = 0.01$, $K = 1 \times 10^8$, $K = 1 \times 10^7$ and $K = 1 \times 10^6$.

result quoted by Orszag [13] in his study of Poiseuille flow over rigid boundaries.

A curve of marginal stability in the $(\alpha, Re)$ plane was also generated using $G = 0$ and above values of $K$, $B$ and $T$. This gave a critical Reynolds number of $Re \cong 5800$ which occurs at a wavenumber of $\alpha = 1.02$. Critical values obtained by Orszag [13] are $Re = 5772$, $\alpha = 1.021$. The accuracy of our numerical method can be improved by increasing the number of collocation points. However, higher accuracy is achieved at the expense of a significant increase in computational time. The Orszag [13] results are widely used as a benchmark for validating numerical codes for the Orr–Sommerfeld equation for plane Poiseuille flow. Fig. 1 shows marginal stability curves for $d = 0$, $T = B = K = 1 \times 10^7$ and various values of the buoyancy parameter $G$. It is apparent that an increase in $G$ reduces the critical Reynolds number, that is, it destabilizes the Tollmien–Schlichting instability waves. On the other hand, an increase in negative buoyancy stabilizes the Tollmien–Schlichting instability waves. Note that negative buoyancy is obtained when the temperature difference between the two walls is negative.

The Richardson number in Gage and Reid [8] is related to our buoyancy parameter $G$ through $G = -4Ri$ and consequently $G < 0$ denotes stable stratification and $G > 0$ denotes unstable stratification. Thus, the results presented in Fig. 1 are in line with the conclusions drawn by Gage and Reid [8] and later by Gage [7].

In Fig. 2 we show the marginal stability curve for fixed values of $T$, $B$, $G$ and varying values of $K$. Fig. 2 shows that when the wall compliance is increased (by reducing the magnitude of a compliant wall parameter) the critical Reynolds number also increases. A similar trend was observed when $B$ was varied keeping $T$, $K$ and $d$ constant, and when $T$ was varied keeping $B$, $K$ and $d$ constant. In Table 1 we present a summary of the results of Fig. 2. Table 1 gives the critical values at which unstable modes begin to exist for various compliant wall parameters when $G = 0.01$, $d = 0$ and $Pr = 1$. This illustrates that wall compliance stabilizes the Tollmien–Schlichting instability waves thus confirming results from earlier studies on compliant channel flows (for example [4,14]).

The difference between the present results and earlier reported results is that increasing the wall compliance does not shrink the marginal stability curve in the range of the Reynolds numbers given in the marginal stability curves. In previous studies on similar plane channel

Table 1
Critical values of $Re$, $\alpha$ for $G = 0.01$, $B = T$ and $d = 0$

| $K$ | $T$ | $\alpha^*$ | $Re^*$ ($\times 10^4$) |
|---|---|---|---|
| $1 \times 10^8$ | $1 \times 10^7$ | 1.0229 | 4827.3 |
| $1 \times 10^7$ | $1 \times 10^7$ | 0.9940 | 4936.6 |
| $1 \times 10^6$ | $1 \times 10^6$ | 0.8257 | 5945.9 |

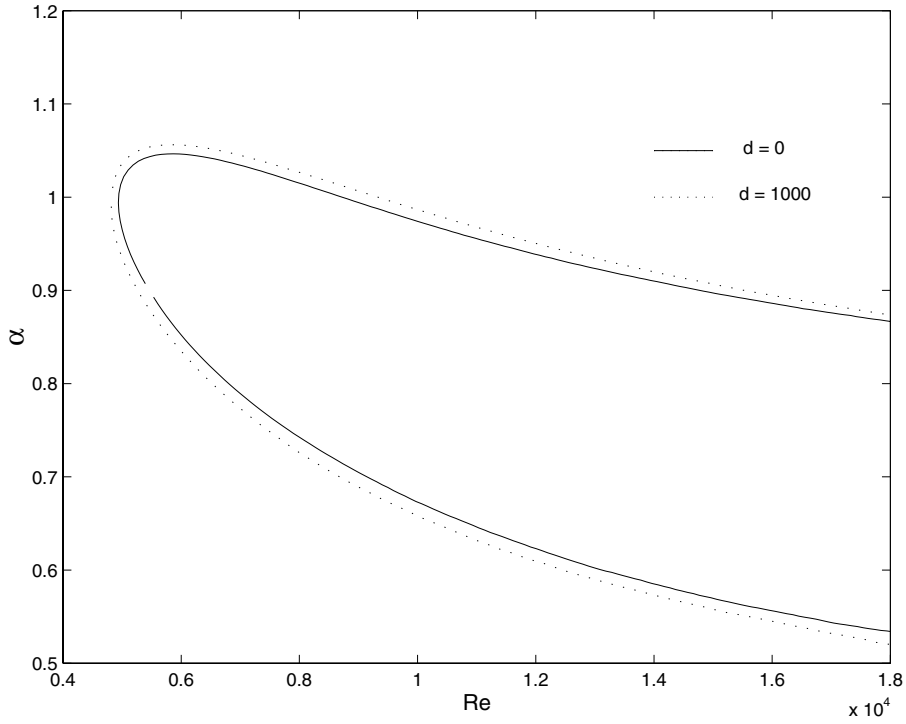


Fig. 3. Marginal stability curve for $T = B = K = 1 \times 10^7$, $G = 0.01$, $d = 0$ (—) and $d = 1000$ (···).

flows over compliant boundaries (see, for example, [4,14]) it was observed that the effect of wall compliance is to shrink the marginal stability curve (within a small range of Reynolds numbers) and cause it to close into a single loop which disappears for sufficiently small values of the wall parameters $T$, $B$ and $K$. This may be attributed to the introduction of buoyancy to the problem which causes the marginal stability curve to start shrinking at very large values of $Re$ (see, for example, Fig. 2 of [8] for the rigid wall case).

The effect of damping is depicted in Figs. 3 and 4 for neutral modes and unstable modes respectively. Damping is seen to slightly destabilize the Tollmien–Schlichting instability waves. Again, this is in agreement with previous studies (see [4]).

In Figs. 5 and 6 we show typical plots of the growth rate of the most unstable mode for fixed values of $G$, $Re$, $Pr$ and compliant wall parameters. The way in which buoyancy and wall compliance affects the maximum growth rate is of great significance because the most rapidly growing mode is likely to dominate in experiments [3]. The real part of the wave speed, $c_r$, represents the oscillations of the velocity perturbations and is another quantity that could be potentially measured in experiments.

Fig. 5 shows the variation of the growth rate against the wavenumber for fixed values of $B$, $K$, $d$, $Re$ and $G$, and varying values of $T$. It is seen that as the tension parameter $T$ is decreased the growth rate also decreases. This shows that an increase in wall compliance leads to the attenuation of the most unstable mode of the Tollmien–Schlichting instability waves. The same trend was observed when $B$ and $K$ were varied, keeping the other parameters fixed.

In Fig. 6 we show the variation of the growth rate against the wavenumber for fixed values of $B$, $K$, $d$, $Re$ and $T$, and varying values of $G$. We note that the growth rate increases as $G$ tends to $+\infty$ and decreases when $G$ tends to $-\infty$.

## 6. Summary

The Chebyshev spectral collocation method has been used to investigate the linear stability of thermally stratified flow in a channel with one compliant wall.

Curves of neutral stability and results showing the variation of the maximum growth rate against the wavenumber were obtained by solving eigenvalue relations. The effect of buoyancy is to destabilize the TS instability waves when $G > 0$ (unstable stratification) and to stabilize the TS instability waves when $G < 0$ (stable stratification). This is in agreement with earlier studies of Gage and Reid [8] and Gage [7].

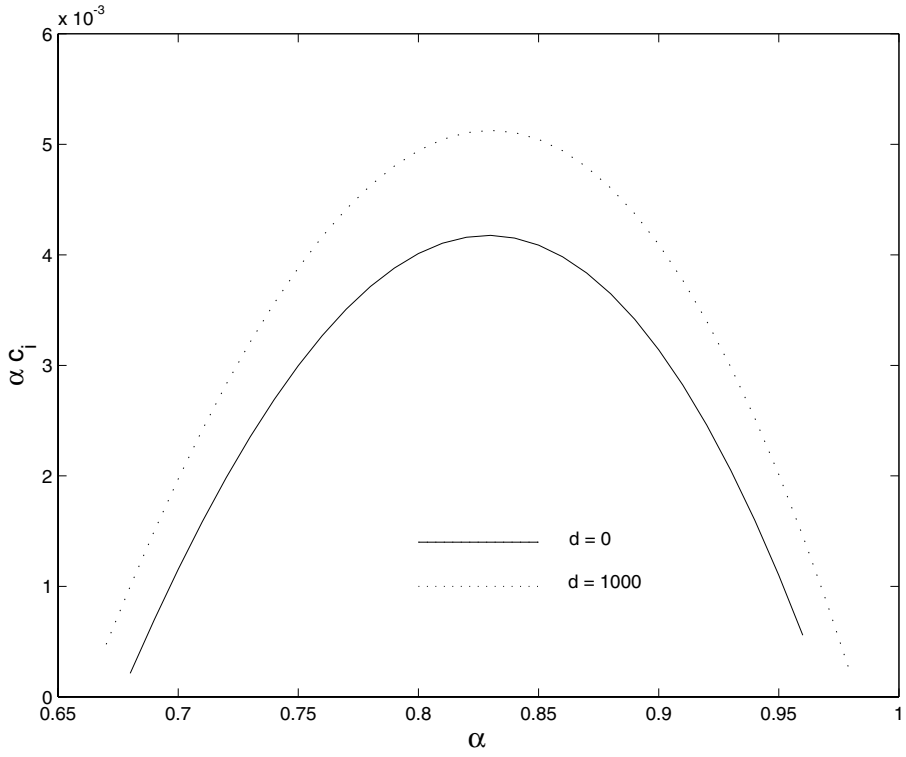


Fig. 4. Wavenumber against growth rate for $Pr = 1$, $Re = 10000$, $B = K = T = 1 \times 10^7$, $G = 0.01$, $d = 0$ (—) and $d = 1000$ ($\cdots$).

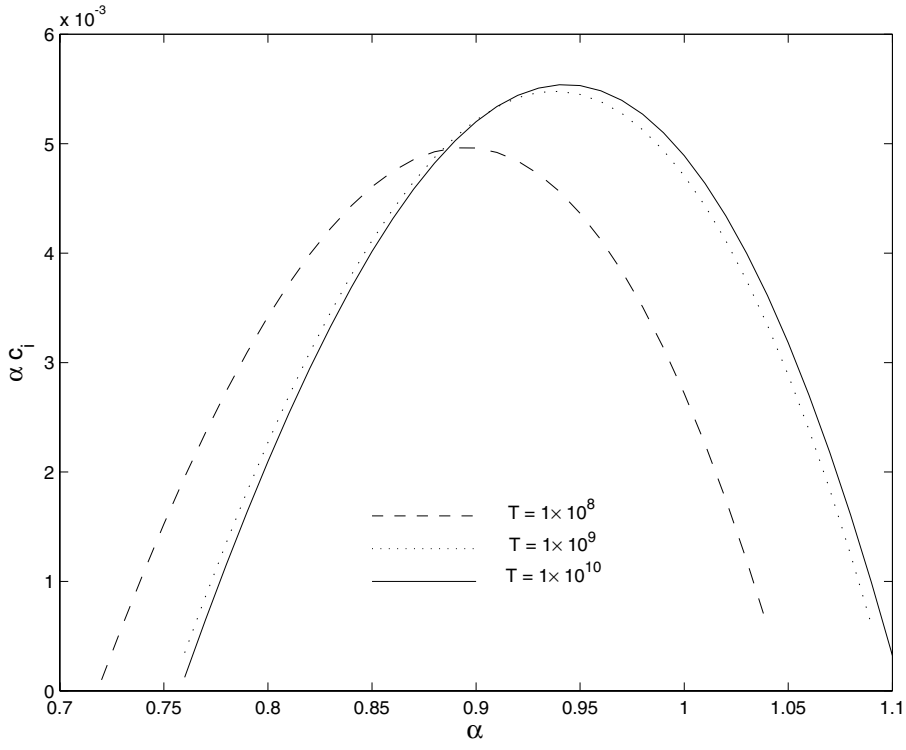


Fig. 5. Wavenumber against growth rate for $G = 0.01$, $Pr = 1$, $Re = 10000$, $B = K = 1 \times 10^6$, $T = 1 \times 10^{10}$, $1 \times 10^9$ and $1 \times 10^8$.

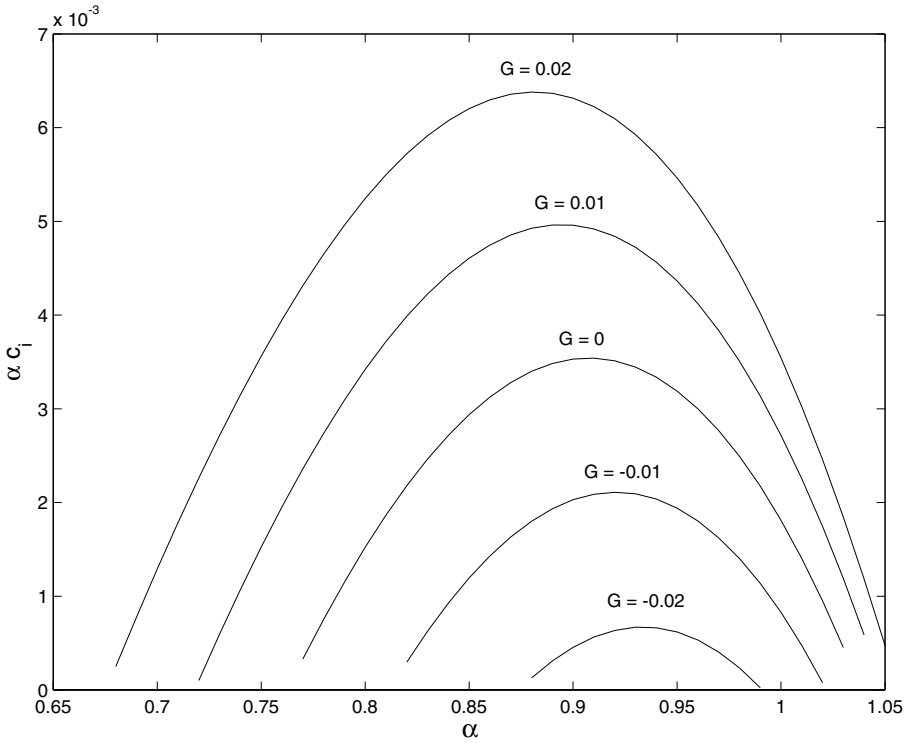


Fig. 6. Wavenumber against growth rate for $Pr = 1$, $Re = 10000$, $d = 0$, $B = K = 1 \times 10^6$, $T = 1 \times 10^8$, $G = -0.02, -0.01, 0, 0.01, 0.02$.

The effect of wall compliance was found to be qualitatively similar to the case when heat transfer is not considered. In particular, it was observed that an increase in the compliance of the wall (for example, decreasing the tension $T$ or the the spring stiffness $K$) is stabilizing and damping is weakly destabilizing for the TS waves.

## Acknowledgements

SSM gratefully acknowledges the financial support from the Norwegian Council of Universities Committee for Cooperation Research and Development (NUFU).

## References

[1] C. Canuto, M.Y. Hussaini, A. Quarteroni, T. Zang, Spectral methods in fluid dynamics, Springer-Verlag, New York, 1988.
[2] P.W. Carpenter, A.D. Garrad, The hydrodynamic stability of flow over Kramer type compliant surfaces. Part 1. Tollmien–Schlichting instabilities, J. Fluid Mech. 155 (1985) 465–510.
[3] A.J. Cooper, P.W. Carpenter, The stability of rotating-disc boundary-layer flow over a compliant wall. Part 1. Type I and II instabilities, J. Fluid Mech. 350 (1997) 231–259.
[4] C. Davies, P.W. Carpenter, Instabilities in plane channel flow between compliant walls, J. Fluid Mech. 352 (1997) 205–243.
[5] J.P. Denier, A.P. Bassom, Neutrally stable wave motions in thermally stratified Poiseuille–Couette flow, J. Austral. Math. Soc. Ser. B 40 (1998) 123–144.
[6] J.P. Denier, E.W. Mureithi, Weakly nonlinear wave motions in a thermally stratified boundary layer, J. Fluid Mech. 315 (1996) 293–316.
[7] K.S. Gage, The effect of stable thermal stratification on the stability of viscous parallel flows, J. Fluid Mech. 47 (1971) 1–20.
[8] K.S. Gage, W.H. Reid, The stability of thermally stratified plane Poiseuille flow, J. Fluid Mech. 33 (1968) 21–32.
[9] J.S.B. Gajjar, P. Sibanda, The hydrodynamic stability of channel flow compliant boundaries, Theoret. Comput. Fluid Dyn. 8 (1996) 105–129.
[10] H. Herwig, The effect of variable properties on momentum and heat transfer in a tube with constant heat flux across the wall, Int. J. Heat Mass Transfer 28 (2) (1985) 423–431.
[11] H. Herwig, P. Schäfer, Influence of variable properties on the stability of two-dimensional boundary layers, J. Fluid Mech. 243 (1992) 1–14.
[12] D. Koppel, On the stability of flow of a thermally stratified fluid under the action of gravity, J. Math. Phys. 5 (1964) 963–982.

[13] S.A. Orszag, Accurate solution of the Orr–Sommerfeld stability equation, J. Fluid. Mech. 50 (Part 4) (1971) 689–703.
[14] J.M. Rotenberry, Finite amplitude shear waves in a channel with compliant boundaries, Phys. Fluids A 4 (2) (1992) 270–276.
[15] J.M. Rotenberry, P.G. Saffman, Effect of compliant boundaries on weakly nonlinear shear waves in channel flow, SIAM J. Appl. Math. 50 (2) (1990) 361–394.
[16] P. Schäfer, N. Herwig, Stability of plane Poiseuille flow with temperature dependent viscosity, Int. J. Heat Mass Transfer 36 (9) (1993) 2441–2448.
[17] P. Schäfer, J. Severin, N. Herwig, The effect of heat transfer on the stability of laminar boundary layers, Int. J. Heat Mass Transfer 38 (10) (1995) 1855–1863.
[18] J. Severin, H. Herwig, Onset of convection in the Rayleigh-Bénard flow with temperature dependent viscosity: An asymptotic approach, Z. Angew. Math. Phys. 50 (1999) 375–386.